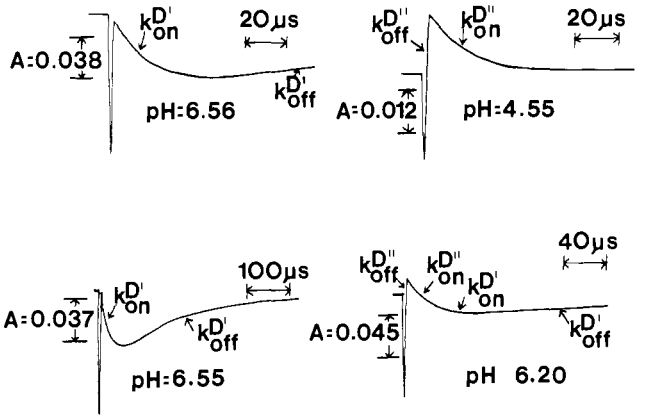

Figure 13. Transient absorbance changes at 640 nm (left-hand-side traces) and at 615 nm (right-hand-side traces) of 4.0×10^{-5} M bromothymol blue in 0.01 M NaCl in the presence of 8.0×10^{-3} M CTAB following a laser pH-jump initiated proton ejection.

Table VI. Rate Constants for Laser pH-Jump Initiated Proton Transfer Involving Indicators in 8.0×10^{-3} M CTAB at 25.0 °C[a]

indicator[b]	pH range	$k_{on}^{D''}$, M^{-1} s^{-1} [c]	$k_{off}^{D''}$, s^{-1} [d]
bromophenol red	3.44–4.45	$(1.61 \pm 0.69) \times 10^9$	2.3×10^4
bromothymol blue	4.54–5.60	$(3.33 \pm 1.0) \times 10^9$	$\times 10^3$

[a] See Scheme I for notations. [b] Stoichiometric concentrations of indicators ranged from (1 to 4) $\times 10^5$ M. [c] Experimentally determined values. Mean of at least six determinations in the indicated pH range. Each value was obtained by following the decay of absorbance due to D'' (at 585 nm for bromophenol red and at 615 nm for bromothymol blue) or the buildup of absorbance due to $D''H^+$ (at 425 nm for bromophenol red and at 418 nm for bromothymol blue). [d] Values calculated from $k_{off}^{D''}/k_{on}^{D'} = K_a$ using the pK_a values given in Table III.

both processes are observable. The small fast initial rise of absorbance at 615 nm, due to the buildup of D'' from $D''H^+$, is attributed to $k_{off}^{D''}$. The subsequent decay is the protonation of D' and D'', governed by $k_{on}^{D'}$ and $k_{on}^{D''}$, followed by a slower recovery of the absorbance by deprotonation, $k_{off}^{D'}$ (Figure 13). At pH 4.55 PO^- protonation, governed by $k_{off}^{D''}$, and subsequent D'' reprotonation, $k_{on}^{D''}$, are the only observable processes. Table VI collects the rate constants determined when PO^- protonation prevailed.

It is important to note that proton transfer to PO^- from any protonated dye could not be observed under any conditions in homogeneous solutions. Apparently, the close proximity of proton donors and acceptors on the positively charged micellar surface is an essential requirement for this process.

Conclusion

Data obtained in this work is consistent with the strong solubilization of the initially formed POH–CTAB complex by micelles. POH, however, remains in a relatively aqueous environment where its rotation is relatively free. Essentially a similar situation has been encountered in the interaction of rose bengal with aqueous micelles.[33] These data are, of course, consistent with current ideas about micellar structures which allow for extensive exposure of the hydrocarbon tails to water.[17]

The identical ground and excited state dissociation of POH in the absence and in the presence of micelles are the consequence of approximately equal retardation of both the protonation and deprotonation rates. These micellar retardation of proton-transfer rates are the consequence of altered microenvironments and electrostatic interactions. If dyes having appropriate pK_a values are solubilized in addition to POH on the micellar surface, the direction of the laser-initiated proton flow can be delicately tuned by altering the pH. Since each micelle contains less than one donor and acceptor, proton transfer must occur via solvent molecules.

Acknowledgment. Support of this work by NSF and ARO is gratefully acknowledged. We thank Mr. Wayne Reed for his continuous help in theoretical and practical matters. M. J. Politi thanks CNPq, Brazil, for a fellowship.

Registry No. POH, 27928-00-3; bromocresol green, 76-60-8; bromophenol red, 2800-80-8; bromothymol blue, 76-59-5; thymol blue, 76-61-9; pyranine, 6358-69-6.

(30) Sager, A.; Maryott, A. A.; Schooley, M. R. *J. Am. Chem. Soc.* **1948**, *70*, 732–736.
(31) "Lange's Handbook of Chemistry"; Dean, J. A., Ed.; McGraw-Hill: New York, 1979; pp 5–86.
(32) Mukerjee, P.; Banerjee, K. *J. Phys. Chem.* **1964**, *68*, 3567–3574.
(33) Reed, W.; Politi, M. J.; Fendler, J. H. *J. Am. Chem. Soc.* **1981**, *103*, 4591–4593.

Dissociation Dynamics of Energy-Selected Hexamethyldisilane Ions and the Heats of Formation of $(CH_3)_3Si^+$ and $(CH_3)_3Si$

Laszlo Szepes[†] and Tomas Baer*

Contribution from the Department of Chemistry, University of North Carolina, Chapel Hill, North Carolina 27514. *Received April 4, 1983*

Abstract: The photoelectron–photoion coincidence (PEPICO) technique has been used to investigate the unimolecular decomposition of the $(CH_3)_6Si_2^+$ molecular ion. The absolute rates of $C_3H_9Si^+$ and $C_5H_{15}Si_2^+$ ion formation were measured as a function of the internal energy by analyzing the ion time-of-flight distribution. The results are compared to the rates predicted by the statistical theory (RRKM/QET). The two dissociation channels are in competition with each other, and their observed onsets are subject to a considerable kinetic shift which is taken into account in evaluating the thermochemical dissociation limits. The rate data show that methyl loss is associated with a tighter transition state than the complex producing $C_3H_9Si^+$ ions. The $\Delta H_f°_{298}$ (in kJ/mol) for the following species were measured: Me_3Si (−49); Me_4Si (−226.2); Me_3Si^+ (629.7); $Me_2Si_2^+$ (423). A Si–Si bond energy of 265 kJ/mol is derived from the heat-of-formation data.

The trimethylsilyl ion is particularly important in the mass spectrometry of methylsilanes, polymethylsilanes, and siloxanes as well as silylated compounds.[1] This ion has been investigated by several authors, and its thermochemistry has been the subject

[†] Department for General and Inorganic Chemistry, Eötvös Loránd University, Budapest, Hungary.

(1) Litzow, M. R.; Spalding, T. R. In "Mass Spectroscopy of Inorganic and Organometallic Compounds"; Elsevier, Amsterdam, 1973; Chapter 7.

0002-7863/84/1506-0273$01.50/0

Table I. Experimentally Observed Ionization and Fragment Appearance Energies in eV

molecule	ion	298 K onset	0 K onset	lit. values
Me_6Si_2	$Me_6Si_2^+$	8.27 ± 0.05[a]	8.27 ± 0.05	UPS: 8.0 (8)
				EI: 8.46 (4); 8.35 (5); 8.79 (9)
	$Me_5Si_2^+$		9.57 ± 0.1[b]	EI: 10.74 (9)
	Me_3Si^+		9.77 ± 0.1[b]	EI: 10.22 (5); 10.25 (4); 10.69 (9)
Me_4Si	Me_3Si^+	10.09 ± 0.01[c]	10.28 ± 0.01	PI: 10.03 (6); 10.09 (3)
Me_3SiCl	Me_3SiCl^+	10.65 ± 0.02[c]	10.83 ± 0.02	EI: 11.00 (9); 10.6 (10)
Me_3SiBr	Me_3Si^+	10.51 ± 0.01[c]	10.70 ± 0.01	EI: 10.69 (9); 10.5 (10)
	Me_2SiBr^+	10.60 ± 0.01[d]	10.79 ± 0.01	EI: 10.7 (10)
Me_3SiI	Me_3Si^+	9.68 ± 0.01[c]	9.87 ± 0.01	EI: 10.1 (10)

[a] Values determined from photoionization efficiency onsets. [b] Value determined from RRKM/QET fit to rate data. [c] Crossover energy (C_{298}) determined from breakdown diagram. [d] Onset estimated by using the difference between Me_3Si^+ and Me_2SiBr^+ onsets.

of a number of studies.[2-13] Some obvious sources for obtaining trimethylsilyl ions are the ionization of the trimethylsilyl radical itself and the dissociative ionization of tetramethylsilane and hexamethyldisilane (HMDS) in which no rearrangement or other unfavorable reactions precede its production. Of these, only tetramethylsilane has been investigated by photoionization. The mass[4,5] and photoelectron[14,15] spectra of HMDS have been well studied so that the fragmentation pathways as well as the ion states are reasonably well understood. However, no attempt has been made to investigate the reaction dynamics of trimethylsilyl ion formation from hexamethyldisilane. This type of information can be derived from photoelectron–photoion (PEPICO) experiments.[16] By this technique, parent ions of well-defined internal energy are prepared, and their subsequent unimolecular decomposition is studied. The slowly decaying parent ions yield asymmetric daughter ion time-of-flight (TOF) distributions from which the reaction rates can be determined.

Decay rate measurements can provide evidence for statistical or nonstatistical energy flow in an isolated ion. All of the metastable hydrocarbon ions so far investigated dissociate at rates consistent with those of the statistical theory (RRKM/QET). Because metal–metal bond strengths tend to be weaker than normal C–C or C–H bonds, these bonds may not be strongly coupled to the C–C and C–H bonds. As a result organometallic ions may not dissociate statistically, and studies of the dissociation rates of energy-selected organometallic ions may therefore provide limiting conditions for the applicability of the statistical theory. In this paper we report on the dissociation dynamics of hexamethylsilane by PEPICO. In order to have a consistent set of thermochemical data, we also determined the ionization and fragment ion appearance energies for hexamethyldisilane, tetramethylsilane, and three trimethylsilyl halides.

Experimental Section

A. Materials. HMDS was purchased from PCR Research Chemicals, Inc. Its purity was checked by gas–liquid chromatography (GLC), and a small amount of an unknown contaminant was removed by GLC. Chloro-, bromo- and iodotrimethylsilane are also commercially available and were purchased from Aldrich Chemical Co. Sample handling was performed in a dry nitrogen atmosphere in order to prevent hydrolysis as much as possible.

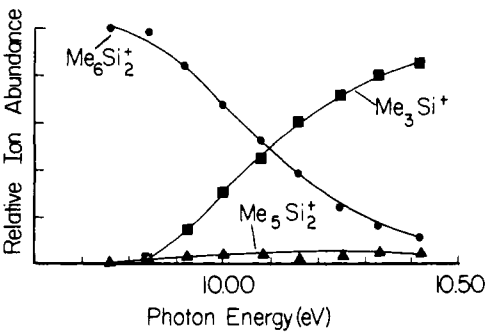

Figure 1. The breakdown diagram of hexamethyldisilane.

B. Threshold Photoelectron–Photoion Coincidence. The photoionization apparatus has been described previously[16-18] so that only the essential features are outlined here. Vacuum UV light from a hydrogen discharge lamp, dispersed with a 1-m normal incidence monochromator, passed through a sample cell pressurized to 1×10^{-4} torr. The resulting photoelectrons and photoions were accelerated in opposite directions by a 12-V/cm electric field. The electrons pass through a steradiancy analyzer which is a filter for low-energy electrons with a resolution of about 35 meV.

The basic principles of photoelectron–photoion coincidence (PEPICO) are as follows: zero kinetic energy electrons are collected in coincidence with parent and fragment ions, so that the ion internal energy is given by $h\nu$ - IE, where IE is the ionization energy. For these experiments a single acceleration region 5 cm in length followed by a 10-cm drift tube are used. The coincidence condition is achieved by using electron and ion signals as start and stop inputs (respectively) to a time-to-pulse height converter whose output is sent to a multichannel pulse height analyzer.

The results from two types of PEPICO experiments are reported here. One is a breakdown diagram which is a plot of the fractional abundance of the ions formed by the dissociation of energy-selected parent ions as a function of the photon energy. This is a plot of the branching ratios to the various dissociation products as a function of the precursor ion internal energy. The breakdown diagrams are obtained directly from a series of PEPICO mass spectra at several photon energies.

In the other type of experiment, lifetimes of metastable ions are measured. Metastable ions of relatively long lifetime dissociate while accelerating in the 12-V/cm electric field. This results in an asymmetric TOF distribution. These distributions can be calculated by using the known ion masses, the accelerating fields and distances, and the one adjustable parameter, the mean ion lifetime. Comparisons between calculated and measured TOF distribution allow ion lifetimes or unimolecular decay rates for energy-selected ions to be determined.

Results

A. Thermochemistry for Breakdown Diagrams. The mass spectrum of HMDS at low ion energy is simple; it contains only parent ions and fragment ions formed by cleavage of Si–Si or Si–C bonds,[4,5] thereby producing the fragment ions Me_3Si^+ and $Me_5Si_2^+$. The breakdown diagram of HMDS is shown in Figure 1. It is evident from this diagram that even though the methyl

(2) Davidson, I. M. T.; Stephenson, I. L. *J. Chem. Soc. A* **1968**, 282.
(3) Distafano, G. *Inorg. Chem.* **1970**, *9*, 1919.
(4) Gaidis, F. M.; Briggs, P. R.; Shannon, T. W. *J. Phys. Chem.* **1971**, *75*, 974.
(5) Lappert, M. F.; Padley, J. B; Simson, F.; Spalding, T. R. *J. Organomet. Chem.* **1971**, *29*, 195.
(6) Murphy, M. K.; Beauchamp, J. L. *J. Am. Chem. Soc.* **1977**, *99*, 2085.
(7) Pietro, W. J.; Pollack, S. K.; Hehre, W. J. *J. Am. Chem. Soc.* **1979**, *101*, 7126.
(8) Potzinger, P.; Ritter, A.; Krause, J. *Z. Naturforsch., A* **1975**, *30A*, 347.
(9) Hess, G. G.; Lampe, F. W.; Sommer, L. H. *J. Am. Chem. Soc.* **1965**, *87*, 5327.
(10) Band, S. J.; Davidson, I. M. T.; Lambert, C. A. *J. Chem. Soc. A* **1968**, 2068.
(11) Block, T. F.; Biernbaum, M.; West, R. *J. Organomet. Chem.* **1977**, *131*, 199.
(12) Green, M. C.; Lappert, M. F.; Pedley, J. B.; Schmidt, W.; Wilkins, B. T. *J. Organomet. Chem.* **1971**, *31*, 55.
(13) Flamini, A.; Semprini, E.; Stefani, F.; Sorriso, S.; Cardaci, G. *J. Chem. Soc., Dalton Trans.* **1976**, *731*.
(14) Bock, H.; Ensslin, W. *Angew. Chem., Int. Ed. Engl.* **1971**, *10*, 404.
(15) Szepes, L.; Korányi, T.; Náray-Szabo, G.; Modelli, A.; Distefano, C. *J. Organomet. Chem.* **1981**, *217*, 35.
(16) Baer, T. In "Gas Phase Ion Chemistry"; M. T. Bowers, Ed.; Academic Press: New York, 1979; Chapter 5.
(17) Butler, J. J.; Baer, T. *J. Am. Chem. Soc.* **1980**, *102*, 6764.
(18) Baer, T.; Willett, G. D.; Smith, D.; Phillips, J. S. *J. Chem. Phys.* **1979**, *70*, 6076.

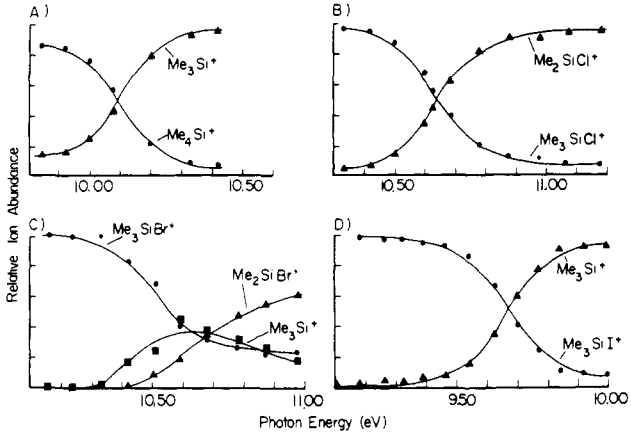

Figure 2. Breakdown diagrams of $(CH_3)_4Si$, $(CH_3)_3SiCl$, $(CH_3)_3SiBr$, and $(CH_3)_3SiI$.

loss product has a lower onset than the Si–Si bond clevage, the former intensity is significantly lower at higher energies. In addition, we note a slow fall off in the parent ion abundance. This is in part a result of the considerable thermal energy in HMDS and in part a result of the slow dissociation which gives rise to a kinetic shift. That is, the observed onsets are shifted to higher energies because the dissociation rates near the thermochemical dissociation limits are too slow to produce sufficient fragments ions to be detected. It is therefore not possible to determine the dissociation limit from the breakdown diagram of HMDS. Under these circumstances it is more meaningful to report the onset of the photoionization efficiency curves for the two fragments. The results of these measurements for the dissociative photoionization of HMDS to $Me_2Si_2^+$ and Me_3Si^+ are listed in Table I. Both onsets are considerably lower than previous electron impact (EI) values.[4,5,9]

In order to determine the $\Delta H_f°$ of the trimethylsilyl ion, we measured the breakdown diagram for tetramethylsilane and the trimethylsilyl halides. As discussed by Baer,[19] if the fragment ion of interest is the first one formed, and there are no complicating factors such as kinetic shift, the crossover point (C_{298}) of the parent and the fragment ion is the energy at which 50% of the parent ions have sufficient energy to dissociate. In the case of Me_3SiCl^+, methyl loss is the lowest energy fragmentation. However, the trimethylsilyl ion is the first fragment formed from tetramethylsilane and bromo- and iodotrimethylsilane parent ions. The breakdown diagrams are shown in Figure 2. The crossover energies, C_{298}, together with ionization onsets (IE) are listed in Table I.

The determination of thermodynamic parameters from the experimentally observed crossover energy, C_{298}, requires a precise definition of the fragment ion appearance energy and a careful analysis of the thermal energy. We summarize the main aspects that have been discussed previously.[19,21-23] To obtain the crossover point, or appearance energy, at 0 K from the experimental value at 298 K, we must add the median thermal internal energy to the C_{298} value. Because the median and average thermal energies are very similar, we used the more readily calculated mean thermal energy to convert C_{298} to C_0. For a dissociative photoionization process

$$AB + h\nu \rightarrow A^+ + B + e^-$$

Table II. Heats of Formation at 0 K and 298 K in kJ/mol[a]

molecule or ion	$\Delta H_f°_0$	$\Delta H_f°_{298}$	$\Delta H_f°_{298}$ (lit. value)
Me_6Si_2	−308.6 ± 8.6[b]		−363 ± 8.6 (20)
Me_4Si	−189.6 ± 4.5[c]	−226.2 ± 4.5[c]	−245 ± 10 (20; −177 (6); −232 (26)
Me_3SiCl	−325.4 ± 3.2[b]		−353.8 ± 3.2 (20)
Me_3SiBr	−258.2 ± 3.5[b]		−293.2 ± 3.5 (20)
Me_3SiI	−189 ± 4[b]		−218 ± 4 (27)
Me_2SiCl^+	574.0 ± 4.0	556.2 ± 4.0	
Me_2SiBr^+	637.2 ± 3.6	611.9 ± 3.6	
$Me_5Si_2^+$	469 ± 10	423 ± 10	
Me_3Si^+	656.3 ± 3.6	629.7 ± 3.6	653 (5); 647.6 (6)
$Me_3Si\cdot$	−22 ± 10	−49 ± 10	−36.1 (5); 10.0 (6)

[a] The $\Delta H_f°_0$ values for the following radicals were taken from ref 25: CH_3 (145.6); Br (117.9); I (107.2). [b] Converted from the 298 K literature value. [c] Data calculated by using $\Delta H_f°_{298}[Me_3Si^+] = 629.7 \pm 4.5$ kJ/mol.

the C_0 of A^+ can be calculated by taking into account the average thermal energy available in dissociating the molecule:

$$C_0 = C_{298} + \langle E_{vib} \rangle + \langle E_{rot.} \rangle$$

Once C_0 is known, it can be expressed in terms of the $\Delta H_f°$ of the various species as:

$$C_0(A^+) = \Delta H_f°_0(A^+) + \Delta H_f°_0(B) + \Delta H_f°_0(e^-) - \Delta H_f°_0(AB)$$

where $\Delta H_f°_0(e^-)$ is zero by definition. To bring the 0 K heat of formation of ion A^+ to 298 K, we use the following thermochemical cycle:

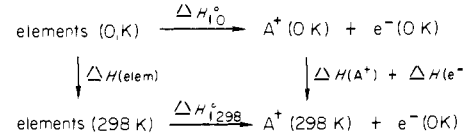

from which $\Delta H_f°_{298}$ can be calculated. We have chosen the NBS convention[21] of setting $\Delta H(e^-) = 0$ at both 0 K and 298 K. The fragment ion, A^+, is treated as an ideal gas, so that $\Delta H(A^+)$ is easily calculated as

$$\Delta H(A^+) = \langle E_{ther} \rangle + RT = \langle E_{vib} \rangle + \langle E_{rot.} \rangle + \langle E_{tran} \rangle + RT$$

in order to calculate $\langle E_{vib} \rangle$ the vibrational partition function has to be evaluated, using the complete set of vibrational frequencies for each species which usually are not available and must be approximated. $\langle E_{rot.} \rangle$and $\langle E_{tran} \rangle$ are obtained by using the classical ideal gas values. In calculating ΔH(elem), $C_P\,dT$ integrals from 0 to 298 K have to be evaluated for all the elements.[24]

Table I lists the calculated C_0 values while Table II summarizes the derived $\Delta H_f°_0$ and $\Delta H_f°_{298}$ values. In the case of HMDS, the kinetic shift prevented the use of the crossover point for determining the thermochemical onset of fragments from HMDS. Therefore the dissociation limits to Me_3Si^+ and $Me_5Si_2^+$ were obtained from the RRKM fits to the measured dissociation rates, as discussed in the followng section.

B. Dissociation Rates and RRKM/QET Calculations. The hexamethyldisilane parent ion is metastable in the threshold energy range of fragment ions $Me_5Si_2^+$ (m/e 131) and Me_3Si^+ (m/e 73). Unfortunately, the $Me_5Si_2^+$ peak is partially overlapped by the parent ion peak because of insufficient mass resolution. As a result, only the TOF peak shapes of Me_3Si^+ were analyzed quantitatively. The lifetimes were measured by collecting fragment ion TOF

(19) Baer, T. "Chemistry of Ions in the Gas Phase"; Reidel Publishing Co.: Holland, 1983; NATO ASI.
(20) Pedley, J. B; Rylance, J. "Sussex—N.P.L. Computer Analyzed Thermochemical Data: Organic and Organometallic Compounds"; University of Sussex, 1977.
(21) Rosenstock, H. M "Kinetics of Ion–Molecule Reactions"; Ausloos, P., Ed.; Plenum Press: New York, 1979.
(22) Traeger, J. C.; McLaughlin, R. C. *J. Am. Chem. Soc.* **1981**, *103*, 3647.
(23) Fraser-Monteiro, M. L.; Fraser-Monteiro, L.; Butler, J. J.; Baer, T.; Hass, R. J. *J. Phys. Chem.* **1982**, *86*, 739.
(24) "JANAF Thermochemical Tables"; 2nd ed.; 1971; Natl. Bur. Stand. Ref. Data Ser., Natl. Bur. Stand., No. 37.
(25) Rosenstock, H. M.; Draxl, K.; Steiner, B. W.; Herron, J. T. *J. Phys. Chem. Ref. Data, Suppl. 1* **1977**, *6*.
(26) Walsh, R. *Acc. Chem. Res.* **1981**, *14*, 246.
(27) Doncaster, A. M.; Walsh, R. *J. Phys. Chem.* **1979**, *83*, 3037.

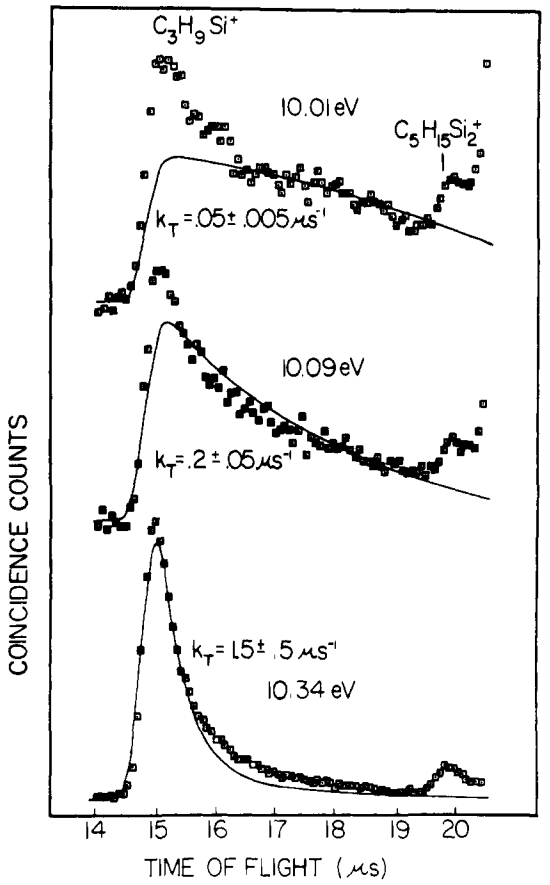

Figure 3. Time-of-flight (TOF) spectra for Me_3Si^+ (m/z 73) and $Me_5Si_2^+$ (m/z 131) at three different photon energies in the metastable energy region.

distributions in coincidence with zero kinetic energy electrons, over a region of ion internal energies ranging from 9.9 to 11.0 eV. Some of the results are shown in Figure 3, in which the points are the experimental data while the solid curves are calculated TOF distribution based on a single unimolecular decay. The experimental TOF distributions at the lower energies clearly exhibit a sharp peak on top of the very asymmetric Me_3Si^+ peak. This peak is actually extremely weak but shows up at low photon energies at which the slow $HMDS^+$ dissociation produces a very weak m/z 73 peak. For the reasons outline below, this sharp peak is attributed to an impurity. A mass spectrum at 9.6 eV, well below the energy at which the m/z 73 peak is apparent, showed two peaks at m/z 72 and 104. The higher mass peak was eliminated after purification by GLC. However, this procedure did not change the amount of the m/z 72 component. Because this peak is symmetric, it can only come from a molecular ion (i.e., impurity), or from a rapid dissociation of the HMDS parent ion. The latter would imply a nonstatistical dissociation, an explanation which is not likely and is not supported by any other findings of this study. We therefore conclude that it arises from an impurity, which is present in minute amounts. Nevertheless, it is evident as a result of the long counting times required near the $HMDS^+$ dissociation threshold.

The experimentally determined rates in Figure 3 are total rates (k_T) of decomposition of the hexamethyldisilane parent ion to all products. If the two dissociation channels are in competition (no isolated states), values of k_T obtained from each fragment peak should be the same at a given photon energy. In our case this requirement could not be checked directly because of partial overlap between peaks of $Me_5Si_2^+$ and $Me_6Si_2^+$ prohibiting the exact analysis of the $Me_5Si_2^+$ metastable peak shape. However, the coincidence data clearly showed (Figure 3) that the $Me_5Si_2^+$ peak is asymmetric at the same energies as the Me_3Si^+ peak. We thus conclude that the two products originate from the same precursor parent ion.

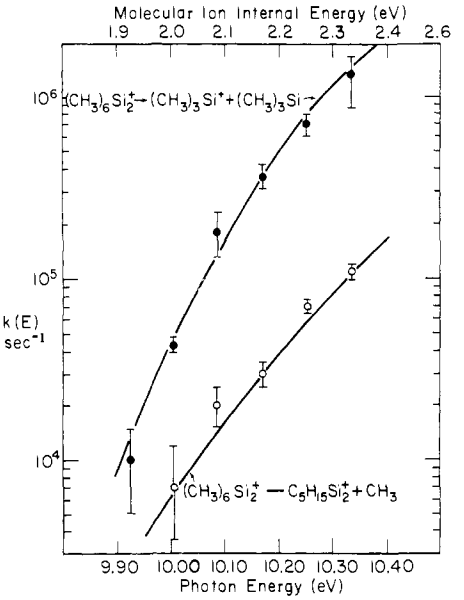

Figure 4. The decay rate, $k(E)$, as a function energy for the dissociation of hexamethyldisilane$^+$ to $Me_3Si^+ + Me_3Si\cdot$ and $Me_5Si_2^+ + Me\cdot$. The solid curves are the results of RRKM/QET calculations using the vibrational frequencies of Table III and activation energies of 1.50 and 1.30 eV respectively for the production of m/z 73 and 131. The upperscale (ion internal energy) is related to the photon energy by the HMDS ionization energy minus the HMDS internal thermal energy, which at 300 K is 0.260 eV.

When different products originate from the same precursor, the total decay rates can be converted into rates of production of the individual fragments by using the ratios of the TOF peak area as ratios of rates to various fragments. This approach has been discussed and applied previously.[18,28] The results are shown in Figure 4 where the points are the experimentally determined rate constants at different photon energies. The $k(E)$ vs. E curve of Me_3Si^+ formation rises more rapidly with a rise in energy than that of the $Me_5Si_2^+$ ion. In terms of RRKM/QET this means a tighter activated state for $Me_5Si_2^+$ formation. On the other hand, by extrapolating to lower energies one can expect a curve crossing resulting in a lower thermochemical threshold for methyl loss.

According to the statistical theory[29,30] (RRKM/QET) the unimolecular decay rate is given by

$$k(E) = \sigma \frac{\int_{\epsilon=0}^{E-E_0} \rho^*(E)\, d\epsilon}{h\rho(E)}$$

where E_0 is the minimum energy needed for reaction, ρ^* and ρ are the densities of internal energy for the transition state and precursor ions, respectively, and σ is a statistical factor equal to the number of independent ways the transition state can be formed. For $k(E)$ to be calculated, E_0 and vibrational frequencies for the transition state and molecular ion must be assumed. For both reactions the vibrational frequencies for the molecular ion were assumed to be those of the neutral molecule.[31,32] By trying various combinations of the other two parameters, best fits shown as solid lines in Figure 4 were found. The best transition-state frequencies for production of m/z 73 and 131 ions together with the molecular ion normal vibrations are listed in Table III. In order to fit the m/z 73 rates, a rather loose transition state with a number of low-frequency vibrations had to be assumed. Two of these can

(28) Willett, G. D.; Baer, T. *J. Am. Chem. Soc.* **1980**, *102*, 6774.
(29) Forst, W. In "Theory of Unimolecular Reactions"; Academic Press: New York, 1973.
(30) The Hase–Bunker program was used with the semiclassical Whitten–Rabinovitch state counting option. This program is available as no. 234 through the Quantum Chemistry Exchange, Inidana University.
(31) Brown, M. P.; Cartmell, E.; Iowles, G. W. A. *J. Chem. Soc.* (*London*) **1960**, 506.
(32) Schumann, H.; Ronecker, S. *Z. Naturforsch., B: Anorg. Chem., Org. Chem., Biochem. Biophys., Biol.* **1967**, *22B*, 452.

Table III. Molecular Ion and Transition-State Vibrational Frequencies Used in the RRKM/QET Calculations

					$Me_6Si_2^+$ Molecular Ion						
2960	2960	2960	2960	2960	2960	2960	2960	2960	2960	2960	2960
2900	2900	2900	2900	2900	2900	1260	1260	1260	1260	1260	1260
1260	1260	1260	1260	1260	1260	1250	1250	1250	1250	1250	1250
1000	1000	1000	1000	1000	1000	1000	1000	1000	1000	1000	1000
900	900	700	700	700	700	650	650	200	200	250	250
250	250	400	200	330	600	220	220	180	180	580	580
					m/z 73 Transition State						
2960	2960	2960	2960	2960	2960	2960	2960	2960	2960	2960	2960
2900	2900	2900	2900	2900	2900	1260	1260	1260	1260	1260	1260
1260	1260	1260	1260	1260	1260	1250	1250	1250	1250	1250	1250
1000	1000	1000	1000	1000	1000	1000	1000	1000	1000	1000	1000
900	900	700	700	700	700	650	650	46	46	46	46
46	46	46	330	600	220	220	180	180	580	580	
					m/z 131 Transition State						
2960	2960	2960	2960	2960	2960	2960	2960	2960	2960	2960	2960
2900	2900	2900	2900	2900	2900	1260	1260	1260	1260	1260	1260
1260	1260	1260	1260	1260	1260	1250	1250	1250	1250	1250	1250
1000	1000	1000	1000	1000	1000	1000	1000	1000	1000	1000	1000
900	900	700	700	700	650	650	100	50	250	250	250
250	400	200	330	600	220	220	180	180	580	580	

be easily justified because two of the Si–Si bending vibrations turn into rotations of the separating products. The origin of the other low frequencies may lie in the increase of the $(Me)_3$–Si solid angle as the transition state is approached. These low frequencies necessary to fit the $k(E)$ curve of Figure 4 are unusual in that the corresponding neutral pyrolysis reaction,[2] measured at 600 K, has a preexponential term of $10^{13.5}$. This implies a small entropy of activation. In contrast, our frequencies for the transition state suggest that the thermal ionic reaction would have a preexponential factor of about 10^{16}. The other variable input parameter was E_0, that is, the minimum energy needed for each reaction. The best values for the E_0's were 1.50 and 1.30 eV for trimethylsilyl and methyl loss, respectively. In both cases, IE + E_0 is considerably lower than the corresponding AE_{obsd} values determined by electron impact (see Table I) or our breakdown curves (Figure 1), thereby indicating a kinetic shift for both reactions. It is also evident that the formation of the $C_5H_{15}Si_2^+$ ion has the lower thermochemical threshold. These findings are also clearly reflected by the breakdown diagram of HMDS shown in Figure 1.

Discussion

The energetics of a number of organosilicon compounds are not well established. Several years ago, Murphy and Beauchamp[6] measured the photoionization efficiency curves for Me_4Si and obtained an onset for methyl loss of 10.03 eV which is very close to our crossover energy of 10.09 eV. However, at that time the $\Delta H_f°$ of tetramethylsilane was not known. The assumed value of −177 kJ/mol, based on electron impact values of silicon compounds,[34] is far higher than the more recently reported values of −245.4 ± 9.9 kJ/mol.[20] and −232 kJ/mol.[26] As a result, the Murphy and Beauchamp value for the Me_3Si^+ heat of formation is considerably higher than ours. However, even the latest values of $\Delta H_f°(Me_4Si)$ are not consistent. This may be because Me_4Si is a rather inert compound so that its heat of formation from reaction with other compounds cannot easily be determined. In addition, the static bomb calorimetry of organosilicon compounds is frustrated by incomplete combustion[33] so that this method is also suspect. Therefore, we can use only the halogen loss onsets in the photoionization of Me_3SiBr and Me_3SiI to provide us with reliable Me_3Si^+ onsets. The more accurately known value for the heat of formation of these two precursors is that of Me_3SiBr. It is determined from the heat of hydrolysis of this molecule which yields a very precise value. The $\Delta H_f°(Me_3SiI)$ is based on equilibrium studies of halogen exchange between Me_3SiBr and Me_3SiI,[27] so that these two values are not independent. The onsets of halogen loss as determined by the breakdown diagrams of Me_3SiBr and Me_3SiI give identical values for the heat of formation of Me_3Si^+ ($\Delta H_f°_{298}$ = 629.7 ± 3.6 kJ/mol). We have used this value along with the onset of methyl loss from Me_4Si to determine a $\Delta H_f°_{298}$ of Me_4Si of −226.2 ± 4.5 kJ/mol, a figure only slightly lower than the latest value of −232 kJ/mol reported by Walsh.[26] It is worth noting that the origin of neither of the two literature values listed in Table II is clear. In one case it is based on unpublished results[26] and in the other case on an unspecified computer retrieval.[20]

A knowledge of the $\Delta H_f°_0(Me_3Si^+)$ and the dissociation onset of Me_3Si^+ from $Me_3SiSiMe_3$ obtained from the RRKM fit to the measured dissociation rates allows us to calculte a $\Delta H_f°_{298}(Me_3Si\cdot)$ of −49.0 ± 10.0 kJ/mol. This is considerably lower than the previously reported value of +10.0 kJ/mol of Murphy and Beauchamp[6] and slightly lower than the −36.1 kJ/mol value of Lappert et al.[5] Because the previous values were either based on an erroneous Me_4Si heat of formation or subject to a kinetic shift in the dissociative ionization of $Me_6SiSiMe_3$, the value based on the present results is considerably more accurate. These energies also allow us to calculate an ionization energy of the trimethylsilyl radical of 7.03 ± 0.10 eV. To our knowledge, there is no direct experimental value for the ionization energy of $Me_3Si\cdot$.

The Si–Si bond energy in HMDS and the Si–C bond energy in Me_4Si can be extracted from the energies of Table II. These are 265 ± 15 kJ/mol and 313 ± 10 kJ/mol, respectively. The Si–C bond energy agrees well with those reported by Davidson and Stephenson[2] of 317 ± 8 kJ/mol and the average bond energy of 309 kJ/mol listed by Lappert et al.[5] However, the Si–Si bond energy is considerably lower than the 281 kJ/mol determined by Davidson and Stephenson in their pyrolysis of HMDS in a static system.[2] The origin of this 0.17-eV discrepancy is not clear. The value from the kinetic study is based on the measured activation energy in a pyrolysis reaction. It assumes that the rate-determining step is the simple bond-cleavage reaction and that the reverse association reaction has no activation energy. Our determination of the Si–Si bond energy (BE) involves a number of thermochemical parameters. Consider the reactions

$$Me_3SiSiMe_3 \rightarrow Me_3Si^+ + Me_3Si \qquad \Delta H_r = AE_0$$

$$Me_3SiSiMe_3 \rightarrow 2Me_3Si \qquad \Delta H_r = BE(Si\text{–}Si)$$

From these we obtain the thermochemical relations

$$\Delta H_f°_0(Me_3Si) = AE_0 - \Delta H_f°_0(Me_3Si^+) + \Delta H_f°_0(Me_3SiSiMe_3)$$

$$BE(Si\text{–}Si) = 2\Delta H_f°_0(Me_3Si) - \Delta H_f°_0(Me_3SiSiMe_3) = 2AE_0 - 2\Delta H_f°_0(Me_3Si^+) + \Delta H_f°_0(Me_3SiSiMe_3)$$

We note that our bond energy depends upon our measured ap-

(33) Cox, F. D.; Pilcher, G. "Thermochemistry or Organic and Organometallic Compounds"; Academic Press: New York, 1970.
(34) Krause, F. R.; Potzinger, P. *Int. J. Mass Spectrom. Ion Phys.* **1975**, *18*, 303.

pearance energy (AE_0) of Me_3Si^+ from HMDS and the heats of formation of Me_3Si^+ and HMDS. Unfortunately, the least accurately known term in the equation for BE(Si–Si) is AE_0, which is multiplied by 2 thereby doubling the uncertainty.

In order to improve on the accuracy of the Si–Si bond energy, we are in need of additional information. The most important and probably easiest method of obtaining this is through the ionization potential of Me_3Si. The Si–Si bond energy is related to the Me_3Si IP and well-known heats of formation via the relation

$$BE(Si–Si) = 2\Delta H_f°_0(Me_3Si^+) - 2IP(Me_3Si) - \Delta H_f°_0(HMDS)$$

The Me_3Si IP is most often quoted or assumed to be about 7 eV. Our BE and AE_0 values yield an IP of 7.03 eV, while the Davidson and Stephenson BE implies an IP of 6.7 eV. Both are reasonable numbers in that they are lower than the measured IP of Me_3C of 7.4 eV.

It is interesting to compare the Si–Si bond energy in HMDS with the C–C bond energy in hexamethylethane. The latter, determined from thermochemical[20] and photoelectron spectroscopic data,[35] is 295.9 kJ/mol. It is thus evident that the Si–Si bond is somewhat weaker than the C–C bond. CNDO/2 calculations show that the $4a_{1g}$ orbital of these compounds has an $\geqslant$M–M$\leqslant$ character (localized bonding) which contributes 48.8% to the bonding in $Me_3C–CMe_3$ and 65.7% in $Me_3Si–SiMe_3$.[15] The higher degree of delocalization of the C–C bond is one of the factors that causes the C–C bond to be stronger than the Si–Si bond.

One of the major aims of this study was to investigate the applicability of the statistical theory to the dissociation of organometallic ions. Our data reveal no inconsistencies with the statistical theory. On the other hand, one might not expect to find nonstatistical energy flow in a molecule such as HMDS whose bond energy is only about 10% weaker than the corresponding C–C analogue. We plan on extending this study to the more metallic tin and germanium analogues in which the metal-to-metal bond energies are considerably less strong, and in which the presence of the heavy atoms may inhibit the free flow of vibrational energy.[36]

Acknowledgment. L. Szepes thanks the CIES for a Fulbright Grant and the University of North Carolina for its hospitality. This work was supported by a grant from the National Science Foundation.

Registry No. Me_6Si_2, 1450-14-2; Me_4Si, 75-76-3; Me_3SiCl, 75-77-4; Me_3SiBr, 2857-97-8; Me_3SiI, 16029-98-4; Me_2SiCl^+, 43641-60-7; Me_2SiBr^+, 43641-30-1; $Me_5Si_2^+$, 87862-42-8; Me_3Si^+, 28927-31-3; $Me_3Si\cdot$, 16571-41-8.

(35) Houle, F. A.; Beauchamp, F. L. *J. Am. Chem. Soc.* **1979**, *101*, 4067.

(36) Lopez, V.; Marcus, R. A. *Chem. Phys. Lett.* **1982**, *93*, 232.

The Ionic Hydrogen Bond. 4. Intramolecular and Multiple Bonds. Protonation and Complexes of Amides and Amino Acid Derivatives

Michael Meot-Ner (Mautner)

Contribution from the Chemical Thermodynamics Division, Center for Chemical Physics, National Bureau of Standards, Washington, DC 20234. *Received August 29, 1983*

Abstract: The thermochemistry of protonation and ion-neutral interactions of $CH_3CON(CH_3)_2$ (DMA) and of the peptide-like alanine derivative $CH_3CONHCH(CH_3)COOCH_3$ (**1**) are models for ionic interactions in proteins. High proton affinity and negative entropy of protonation of **1** vs. DMA indicate intramolecular hydrogen bonding in $\mathbf{1H^+}$. The intermolecular bond in $\mathbf{1H^+}$, i.e., in

$$CH_3\dot{C}OH^+NHCH(CH_3)\dot{C}OOCH_3$$

stabilizes this ion by 7 kcal mol^{-1}. However, the internal hydrogen bond decreases the availability of the proton for external hydrogen bonding. Thus, the attachment energy of H_2O to $\mathbf{1H^+}$, 13.0 kcal mol^{-1}, is lower than that to $DMAH^+$, 16.5 kcal mol^{-1}. The thermochemistry of the $\mathbf{1H^+}\cdot H_2O$ complex suggests a T-shaped structure, or one where H_2O bridges between the two carbonyl groups. In other complexes **1** can serve as a neutral ligand. In such a complex, $CH_3NH_3^+\cdot\mathbf{1}$, the unusually large experimental enthalpy of complexation, −40.1 kcal mol^{-1}, suggests multiple hydrogen bonding. These results, combined with the thermochemistry of protonated amide dimers, suggest that intramolecular and multiple ionic hydrogen bonds can contribute significantly to the stabilities of ionic intermediates in protein and enzyme environments. Such contributions can range, per single hydrogen bond, from 5 kcal mol^{-1} for strained and distorted bonds to 30 kcal mol^{-1} for geometrically optimized bonds.

Many organic and enzymic reactions proceed through protonated intermediates. The proton affinities of complex molecules and the interactions of the protonated species with polar ligands therefore can be important in bioenergetics.[1] This paper examines the proton affinities and ionic hydrogen bonding of some amides and of the N-acetylated amino acid derivative $CH_3CONHCH(CH_3)COOCH_3$, (CH_3CO-Ala-OCH_3, also denoted here as compound **1**). The thermochemistry of these species can serve as a model for the energetics of protonated intermediates in acid hydrolysis of amides and the energetics of protonated amide groups in proteins.

The present paper continues a series of studies on both the intramolecular and intermolecular hydrogen bonding interactions of polyfunctional ions.[2-4] In those studies, the proton affinities, entropies of protonation, and ionic hydrogen bonding of the polyfunctional species are compared with those of model mono-

(1) Warshel, A. *Acc. Chem. Res.* **1981**, *14*, 284.

(2) Yamdagni, R.; Kebarle, P. *J. Am. Chem. Soc.* **1973**, *95*, 3504.

(3) Meot-Ner (Mautner), M.; Hamlet, P.; Hunter, E. P.; Field, F. M. *J. Am. Chem. Soc.* **1980**, *102*, 6393.

(4) Meot-Ner (Mautner), M., *J. Am. Chem. Soc.* **1983**, *105*, 4906, 4912.